Synthesis of a Magnesium/Aluminum/Iron Layered Double Hydroxide and Its Flammability Characteristics in Halogen-Free, Flame-Retardant Ethylene/Vinyl Acetate Copolymer Composites

Chuan-Mei Jiao, Zheng-Zhou Wang, Xi-Lei Chen, Yuan- Hu

State Key Laboratory of Fire Science, University of Science and Technology of China, Anhui 230026, People's Republic of China

Received 20 November 2006; accepted 5 September 2007
DOI 10.1002/app.27393
Published online 13 November 2007 in Wiley InterScience (www.interscience.wiley.com).

ABSTRACT: Mg–Al–Fe ternary hydrotalcites were synthesized by a coprecipitation method and characterized with powder X-ray diffraction, Fourier transform infrared spectroscopy, and thermogravimetric analysis. The flame-retardant effects of Mg/Al–CO_3 layered double hydroxides (LDHs) and Mg/Al/Fe–CO_3 LDHs in an ethylene/vinyl acetate copolymer (EVA) were studied with the limited oxygen index (LOI), the UL-94 test, and the cone calorimeter test (CCT), and the thermal degradation behavior of the composites was examined by thermogravimetric analysis. The results showed that the LOI values of the EVA/(Mg/Al/Fe–CO_3 LDH) composites were basically higher than those of the EVA/(Mg/Al–CO_3 LDH) composites at the same additive level. In the UL-94 test, there was no rating for the EVA/(Mg/Al–CO_3 LDH) composite at the 50% additive level, and a dripping phenomenon occurred. However, the EVA/(Mg/Al/Fe–CO_3 LDH) composites at the same loading level of LDHs containing a suitable amount of Fe^{3+} ion reached the V-0 rating, the dripping phenomenon disappearing. The CCTs indicated that the heat release rate (HRR) of the EVA composites with Mg/Al/Fe–CO_3 LDHs containing a suitable amount of Fe^{3+} decreased greatly in comparison with that of the composites with Mg/Al–CO_3 LDHs. The introduction of a given amount of Fe^{3+} ion into Mg/Al–CO_3 LDHs resulted in an increase in the LOI, a decrease in the HRR, and the achievement of the UL-94 V-0 rating. © 2007 Wiley Periodicals, Inc. J Appl Polym Sci 107: 2626–2631, 2008

Key words: flame retardance; FT-IR; synthesis; thermogravimetric analysis (TGA); X-ray

INTRODUCTION

In recent years, halogen-free flame retardants have been widely used in the flame retardation of polymers because of advantages such as low smoke, no toxicity, and no corrosive gas generation. Many investigations have demonstrated that inorganic hydroxide fillers, especially magnesium hydroxide (MH) and aluminum hydroxide (ATH), are environmentally friendly additives.[1–4] They are extensively used in polymeric materials for manufacturing halogen-free and low-smoke cables. However, they have some disadvantages, such as high loadings and poor compatibility with the polymeric matrix, which degrade the mechanical properties.[5,6] Therefore, it is significant to look for some other inorganic hydroxides to substitute for existing metal hydroxides MH and ATH.

Hydrotalcites have attracted much attention during the development of new environmentally friendly flame retardants.[7–10] Hydrotalcite-like compounds known as layered double hydroxides (LDHs) are a class of anionic clays, whose general formula is $[M^{II}_{1-x}M^{III}_{x}(OH)_2]^{x+}[(Y^{m-})_{x/m}]\cdot nH_2O$, where M^{II} is a divalent metal cation, M^{III} is a trivalent metal cation, and Y stands for m valence inorganic or organic acid anions.[11] The structure of the hydrotalcites is derived from a brucite structure in which trivalent cations partially substitute for divalent ones. Because of their layered structure and high anion-exchange capacity, LDHs are now used in various applications. For example, they can be used as catalysts and catalyst precursors, adsorbents, electrochemicals, hosts for nanoscale reactions, thermal stabilizers, and so on.[12–17] LDHs possess compositions similar to those of MH and ATH and are very promising as halogen-free flame-retardant additives. In our previous work,[8] we studied the flame-retardant behavior of Mg/Al–CO_3 LDHs in an ethylene/vinyl acetate

Correspondence to: Z.-Z. Wang (zwang@ustc.edu.cn).
Contract grant sponsor: National Natural Science Foundation of China; contract grant number: 50273036.
Contract grant sponsor: China National Key Basic Research Special Funds project; contract grant number: 2001CB409600.

copolymer (EVA), and compared the flame-retardant efficiency with that of MH. The flame-retardant efficiency of Mg/Al–CO_3 LDHs was better than that of MH at the same additive level. Moreover, Mg/Al–CO_3 LDHs possessed superior smoke-suppressant performance during the combustion of the EVA composite.

In the flame-retardant field, iron compounds have been known as flame-retardant synergists in halogen systems, but their utility in nonhalogen systems has been largely unrecognized. Nangrani et al.[18] reported that ferric oxide actually increased the flammability of polycarbonate. Whelan[19] investigated iron oxide as an effective synergist with halogens in halogen-containing nitrile polymers. Moreover, Zhu and Wilkie[20] showed that clays containing iron enhanced the thermal stability of polystyrene–clay nanocomposites by thermogravimetric analysis (TGA) or cone calorimetry. Therefore, hydrotalcites containing iron ions probably have higher flame-retardant efficiency in some other flame-retardant systems. In this study, Mg/Al/Fe–CO_3 LDHs were synthesized and characterized, and the flammability characteristics and thermal degradation of EVA/Mg/Al/Fe–CO_3 LDH composites were studied.

EXPERIMENTAL

Materials

EVA28 (containing 28 wt % vinyl acetate) was bought from Sumitomo Chemical Co., Ltd. (Japan) Mg$(NO_3)_2{\cdot}6H_2O$, Al$(NO_3)_3{\cdot}9H_2O$, Fe$(NO_3)_3{\cdot}9H_2O$, NaOH, and Na_2CO_3 were standard laboratory reagents and were used as received without further purification.

Synthesis of hydrotalcite

Mixed salt solutions containing Mg$(NO_3)_2$, Al$(NO_3)_3$, and Fe$(NO_3)_3$ were prepared with Mg/Al/Fe molar ratios of 6.0/2.0/0 (Mg/Al–CO_3 LDH), 6.0/1.75/0.25 (Mg/Al/Fe–CO_3 LDH-A), 6.0/1.5/0.5 (Mg/Al/Fe–CO_3 LDH-B), and 6.0/1.0/1.0 (Mg/Al/Fe–CO_3 LDH-C). Corresponding mixed base solutions containing NaOH and Na_2CO_3 were prepared with $[CO_3^{2-}]/([Al^{3+}] + [Fe^{3+}]) = 2.0$ and $[OH^-]/([Al^{3+}] + [Mg^{2+}] + [Fe^{3+}]) = 1.6$. Each mixed salt solution and its corresponding base solution were simultaneously added to an emulsifying machine with a certain rotor speed and mixed for a certain time. The resulting slurry was transferred into a three-necked flask and aged at 100°C for 6 h. The final precipitate was centrifuged, washed thoroughly, and dried at 100°C for 24 h to obtain Mg/Al–CO_3 LDH or Mg/Al/Fe–CO_3 LDH series.

Preparation of the EVA composites

All compositions were melt-compounded with a two-roll mill at about 120°C for 10 min. After mixing, the mixtures were then compression-molded at about 120°C into sheets (3 mm thick) under a pressure of 10 MPa for 10 min. The sheets were cut into suitably sized specimens for fire testing. In this work, the additive level of all samples was 50%, and the samples were named ELDH-1 (containing 50 wt % Mg/Al–CO_3 LDH without Fe^{3+}), ELDH-2 (containing 50 wt % Mg/Al/Fe–CO_3 LDH-A), ELDH-3 (containing 50 wt % Mg/Al/Fe–CO_3 LDH-B), and ELDH-4 (containing 50 wt % Mg/Al/Fe–CO_3 LDH-C).

Measurements

X-ray diffraction (XRD)

XRD data were recorded at room temperature on a Philips X'Pert Pro Super apparatus (Nicolet Instrument Co., Madison, WI) using Cu Kα radiation with a nickel filter (wavelength = 1.5418 Å) at a scan rate of 0.0167°/s.

Fourier transform infrared (FTIR) spectroscopy

FTIR spectra were recorded with a Nicolet Magna-IR 750 spectrometer and KBr disks.

Limited oxygen index (LOI)

The LOI measurements were carried out with an HC-2 type instrument (Nanjing, China) according to ASTM D 2863. The size of the specimens was 100 × 6.5 × 3 mm^3.

UL-94 test

The vertical test was performed on sheets of 127 × 12.7 × 3 mm^3 according to the UL-94 test standard.

Cone calorimeter test (CCT)

A cone calorimeter (Stanton Redcroft, England) was used to measure the flammability characteristics under a heat flux of 35 kW/m^2 according to ISO 5660. The measured parameters included the heat release rate (HRR), the time to ignition, and so forth.

TGA

The thermogravimetry (TG) experiments were carried out on a DT-50 (Shimadzu, Japan). About 10 mg of a cured sample was put in an alumina crucible

and heated from 25 to 700°C. The test was performed at a heating rate of 10°C/min in air and nitrogen atmospheres at a flow rate of 150 mL/min.

RESULTS AND DISCUSSION

Characterization of the Mg/Al/Fe–CO_3 LDH series

XRD characterization of the Mg/Al/Fe–CO_3 LDH series

XRD patterns of the Mg/Al/Fe–CO_3 LDH series with different Mg/Al/Fe molar ratios are shown in Figure 1. All the diffraction peaks are in good agreement with layered structures and are ascribable to LDHs indexed in a hexagonal lattice. Figure 1 shows that the diffraction peaks are sharp, being indicative of relatively well-formed crystalline layered structures. Moreover, the diffraction peak position of the crystal plane (110) is different for four kinds of LDH samples. The 2θ value shifts to a lower angle with an increase in the amount of Fe^{3+} contained in the LDHs. The explanation for the change in the position of the (110) crystal plane is that d_{110} reflects the array density of atoms on the veneer sheet, and cell parameter a becomes smaller when the array density of atoms on the veneer sheet increases. The smaller a is, the smaller d_{110} is. In the Mg/Al/Fe–CO_3 LDHs, because the radius of Fe^{3+} is larger than that of Al^{3+}, the array density of atoms on the veneer sheet of Mg/Al/Fe–CO_3 LDH is smaller than that of Mg/Al–CO_3 LDH. Unit cell parameter a increases with increasing isomorphous substitution of Al^{3+} by Fe^{3+}, and the value of d_{110} increases with the increase in the amount of Fe^{3+}; thus, the position of the (110) crystal plane shifts to a lower 2θ angle.

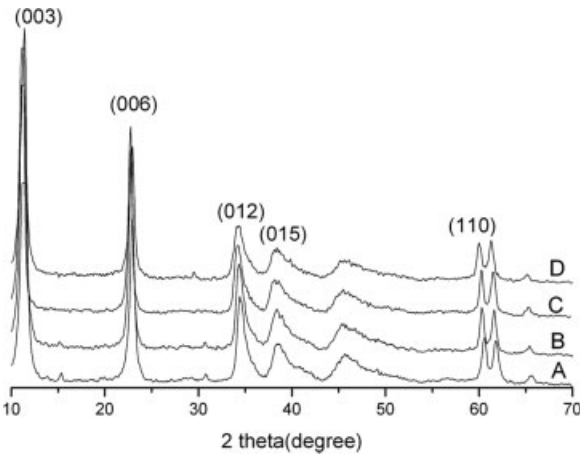

Figure 1 XRD patterns of the Mg/Al/Fe–CO_3 LDH series: (A) Mg/Al–CO_3 LDH, (B) Mg/Al/Fe–CO_3 LDH-A, (C) Mg/Al/Fe–CO_3 LDH-B, and (D) Mg/Al/Fe–CO_3 LDH-C.

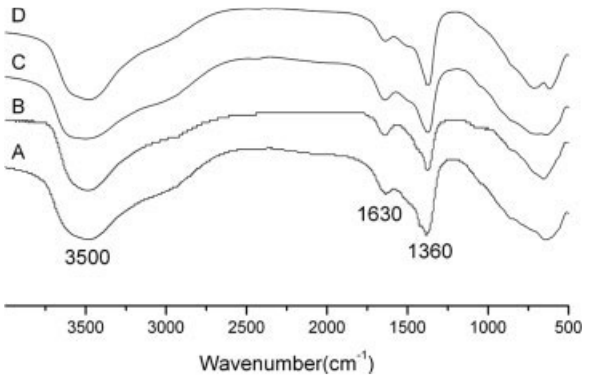

Figure 2 FTIR spectra of the Mg/Al/Fe–CO_3 LDH series: (A) Mg/Al–CO_3 LDH, (B) Mg/Al/Fe–CO_3 LDH-A, (C) Mg/Al/Fe–CO_3 LDH-B, and (D) Mg/Al/Fe–CO_3 LDH-C.

FTIR characterization of the Mg/Al/Fe–CO_3 LDH series

The FTIR spectra of a series of Mg/Al/Fe–CO_3 LDHs samples are shown in Figure 2. The broad band around 3500 cm^{-1} can be ascribed to the stretching mode of hydroxyl groups attached to metal ions of Mg, Al, and Fe in the layers, and the band close to 1630 cm^{-1} is assigned to the bending vibration of interlayer water molecules. The narrower absorption peak at 1360 cm^{-1} is attributed to the asymmetric ν_3 vibration of interlayer CO_3^{2-}. The shape and position of the three aforementioned peaks experience no obvious change with different molar ratios of Mg, Al, and Fe in the layers. Bands at lower wave numbers (620–690 cm^{-1}) might be attributed to the overlap of the asymmetric ν_4 vibration modes of CO_3^{2-} and the stretching vibrations including M–O, M–O–M, and O–M–O bands in the layer. For Mg/Al–CO_3 LDH and Mg/Al/Fe–CO_3 LDH-A, there is only one peak in the range of 620–690 cm^{-1}. However, as the amount of Fe^{3+} ion increases in the LDHs, the single peak changes into two peaks in the range of 620–690 cm^{-1}, and the position of the vibration peaks attributed to M–O, M–O–M, and O–M–O bands slightly changes. The explanation of the change in the position of the peak is that the isomorphous substitution of Al^{3+} by Fe^{3+} leads to the change in the element on the veneer sheet. The different radii of atoms make the density of charge on the veneer sheet change. Therefore, the stretching vibrations of M–O, M–O–M, and O–M–O slightly change.

TG behavior of the Mg/Al/Fe–CO_3 LDH series

Figure 3 presents the TG and differential thermogravimetry (DTG) curves of Mg/Al/Fe–CO_3 LDH series with different molar ratios of Mg, Al, and Fe. It can be seen from Figure 3 that four kinds of Mg/Al/Fe–CO_3 LDHs all exhibit a two-step weight-loss

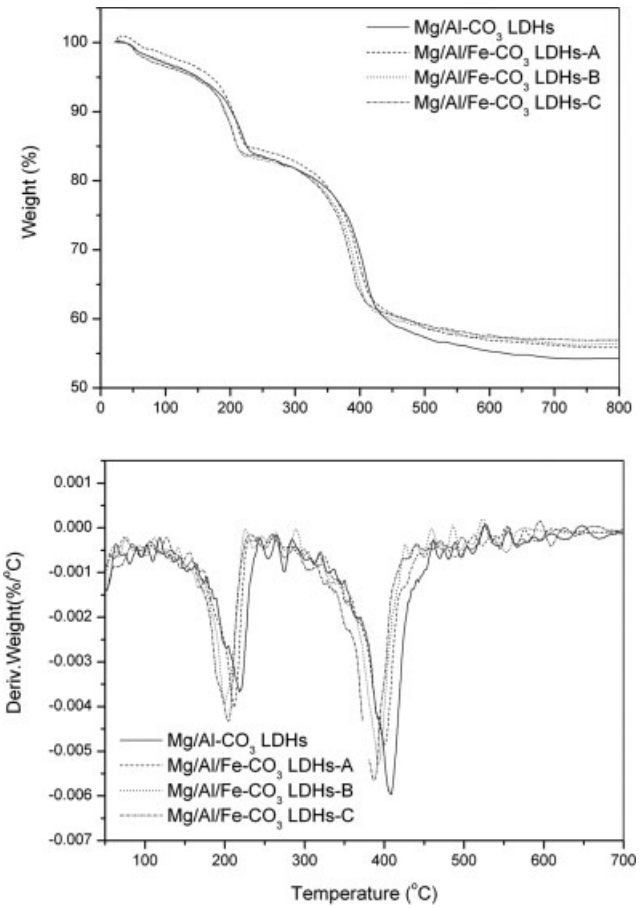

Figure 3 TG and DTG curves of the LDH series.

process. The first step below 250°C is attributed to the loss of loosely bound water in the interlayer space, with the temperature at the maximum rate of weight loss (T_{max}) in the range of 215–205°C. The second step starts above ~ 250°C and belongs to the simultaneous dehydroxylation and decarbonation of the lattice, and T_{max} at this step is in the range of 405–390°C. The T_{max} values are different when the molar ratio of Mg, Al, and Fe in the LDHs changes, and the isomorphous substitution of Al^{3+} by Fe^{3+} reduces the mass-loss temperature of Mg/Al/Fe–CO_3 LDHs at the same weight-loss level, T_{max} shifting to a lower temperature as the amount of Fe^{3+} in the LDHs increases. Moreover, above 800°C, the amount of residue left after the degradation is different for the Mg/Al/Fe–CO_3 LDH series, and the value increases with the increase in the amount of Fe^{3+}.

Combustion behavior of the EVA/LDH composites

Effect of LDHs on the LOI values and UL-94 rating of the EVA/LDH composites

Table I presents the effects of Mg/Al/Fe–CO_3 LDHs on the LOI values and UL-94 test results of EVA/LDH composites. Compared with LOI of control sample ELDH-1 (EVA/Mg/Al–CO_3 LDH), the LOI values of EVA/(Mg/Al/Fe–CO_3 LDH) composites first increase and then decrease slightly with the increase in the amount of Fe^{3+} ion. For example, the LOI value of sample ELDH-2, containing a 50% loading level of Mg/Al/Fe–CO_3 LDH-A, increases to 38.0% from 36.0% (sample ELDH-1). When the same loading level of Mg/Al/Fe–CO_3 LDH-B is added to EVA, the LOI value of sample ELDH-3 increases to 41.2%. However, the LOI value of sample ELDH-4 decreases to 35.0% with a higher amount of Fe^{3+}. Moreover, the introduction of Fe^{3+} into LDHs can prevent the EVA/(Mg/Al/Fe–CO_3 LDH) composites from dripping and improve the UL-94 rating, as shown in Table I. At the same loading level, a dripping phenomenon occurs for control sample ELDH-1 during the UL-94 testing, whereas no dripping is observed for samples ELDH-2 and ELDH-3. In addition, sample ELDH-3 with Mg/Al/Fe–CO_3 LDH-B can extinguish itself after ignition and reaches the UL-94 V-0 rating. These results indicate that the introduction of Fe^{3+} into LDHs can greatly enhance the flame-retardant efficiency of LDHs in EVA/LDH composites. The improvement of the flame-retardant efficiency by the introduction of Fe^{3+} into LDHs probably occurs because Fe^{3+} ions possessing catalysis activity accelerate the formation of a char layer and trap free radicals during the combustion.

Dynamic HRR of the EVA/LDH composites

The CCT, based on the oxygen consumption principle, has now been extensively used to evaluate the flammability of polymer materials because its results correlate well with those obtained from large-scale fire tests. The dynamic HRR curves of the EVA/LDH composites containing different kinds of Mg/Al/Fe–CO_3 LDHs with a 50 wt % loading level are shown in Figure 4. The peak HRR values of EVA/(Mg/Al/Fe–CO_3 LDH) composites decline compared with those of the EVA/(Mg/Al–CO_3 LDH) composite. For example, the peak HRR value of sample ELDH-3 is lower than that of sample ELDH-1, the value decreasing from 387 to 277 kW/m^2. Moreover, the combustion process is prolonged, and the time of the peak of the HRR appearance is delayed. How-

TABLE I
LOI Values and UL-94 Test Results for EVA/LDH Composites

Sample code	LOI (%)	UL-94 rating	Phenomenon
ELDH-1	36.0	Fail	Dripping
ELDH-2	38.0	Fail	No dripping
ELDH-3	41.2	V-0	No dripping
ELDH-4	35.0	Fail	Dripping

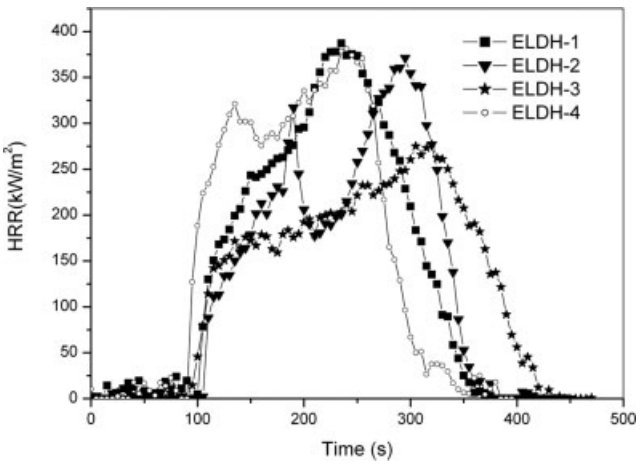

Figure 4 Dynamic HRR curves of the EVA composites with different kinds of LDHs.

ever, when the Mg/Al/Fe–CO_3 LDHs contain a higher concentration of Fe^{3+}, the peak HRR value of the EVA/(Mg/Al/Fe–CO_3 LDH) composite (sample ELDH-4) increases.

TG behavior of the EVA/LDH composites

Figure 5 shows the TG curves of samples ELDH-1, ELDH-3, and ELDH-4 in an atmosphere of air. It can be seen that the decomposition of the three EVA composites includes three weight-loss steps. The first step of the composites is attributed to the loss of loosely bound water in the interlayer space of LDHs in the composites. The second and third steps belong to the simultaneous dehydroxylation and decarbonation of the lattice of LDHs, which overlap with the decomposition of the acetate groups in EVA side chains and the scission of the main chains of EVA. In the first and second weight-loss stages, the TG curves of ELDH-3 and ELDH-4 composites shift to a lower temperature compared with the curve of the ELDH-1 composite at the same weight loss. It is interesting to find that when the temperature is in the range of 480–560°C, the TG curves of ELDH-3 and ELDH-4 composites shift to a higher temperature compared with the curve of the ELDH-1 composite. The decrease in the thermal stability of the first and second weight-loss stages is probably attributable to two factors. First, the thermal stability of Mg/Al/Fe–CO_3 LDHs in the first two stages is lower than that of Mg/Al–CO_3 LDHs. Second, the action of Fe^{3+}-ion catalysis activity promotes the degradation of EVA resin. Moreover, the action of Fe^{3+}-ion catalysis activity also promotes the formation of a char layer to enhance the thermal stability in the temperature range of 480–560°C. Contrary to our expectations, the amount of residue left at 800°C is not enhanced by the presence of Fe^{3+} ions in Mg/Al–CO_3 LDHs. The TG results of samples ELDH-1, ELDH-3, and ELDH-4 in N_2 also indicate that the amount of residue left at 800°C for the composites with Fe^{3+} ions (ELDH-3 and ELDH-4) is not significantly enhanced by the presence of Fe^{3+} ions compared with that of the composites (ELDH-1) without Fe^{3+} ions (Fig. 6). Combining these results with those for the LOI value, UL-94 test, and HRR value, we can draw the conclusion that an effective flame retardant need not increase the yield of char. Weil and Pate[21] also reported that the mode of action of flame retardants appears connected to improved char morphology rather than quantity. The improvement of the flame-retardant efficiency for LDHs containing Fe^{3+} ions might be due to another mechanism, such as a radical-trapping mechanism of Fe^{3+} ions in the gaseous phase, which needs to be studied further.

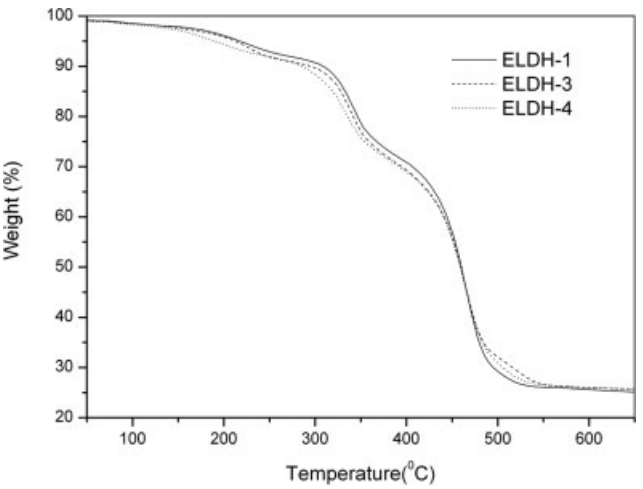

Figure 5 TG curves of samples ELDH-1, ELDH-3, and ELDH-4 in air.

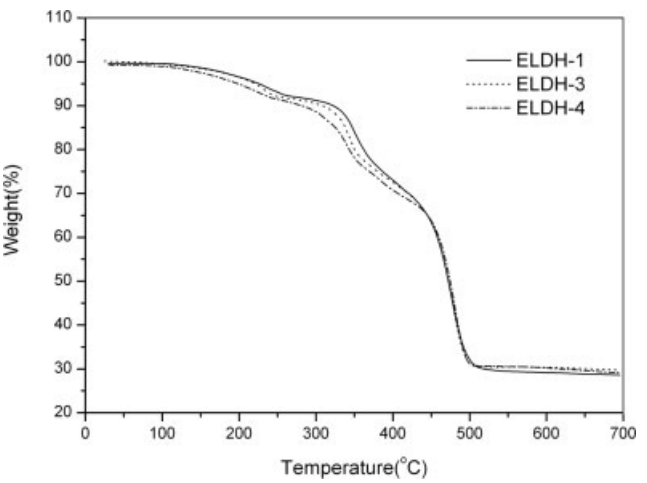

Figure 6 TG curves of samples ELDH-1, ELDH-3, and ELDH-4 in N_2.

CONCLUSIONS

The flammability characteristics and thermal degradation behavior of Mg/Al/Fe–CO_3 LDH series have been compared with those of Mg/Al–CO_3 LDHs in EVA by LOI, UL-94, CCT, and TGA testing. The results show that Mg/Al/Fe–CO_3 LDHs are better than Mg/Al–CO_3 LDHs in improving the flame retardation of EVA at the same additive loading level. The CCT data indicate that the HRR of the ELDH-3 composite is lower than that of the ELDH-1 composite. The LOI value of the ELDH-3 composite is about 5% higher than that of the ELDH-1 composite at the 50% loading level. The results indicate that the introduction of Fe^{3+} into Mg/Al–CO_3 LDHs can improve their flame retardancy in EVA.

References

1. Su, Z. P.; Jiang, P. K.; Li, Q.; Wei, P.; Zhang, Y. Polym Compos 2005, 13, 139.
2. Lv, J. P.; Qiu, L. Z.; Qu, B. J. Nanotechnology 2004, 15, 1576.
3. Fu, M. Z.; Qu, B. J. Polym Degrad Stab 2004, 85, 633.
4. Li, Z. Z.; Qu, B. J. Polym Degrad Stab 2003, 81, 401.
5. Wang, Z. Z.; Qu, B. J.; Fan, W. C.; Huang, P. J Appl Polym Sci 2001, 81, 206.
6. Rothon, R. N.; Hornsby, P. R. Polym Degrad Stab 1996, 54, 383.
7. Camino, G.; Maffezzoli, A.; Braglia, M.; Lazzaro, M. D.; Zammarano, M. Polym Degrad Stab 2001, 74, 457.
8. Jiao, C. M.; Wang, Z. Z.; Ye, Z.; Hu, Y.; Fan, W. C. J Fire Sci 2006, 24, 47.
9. Jiao, C. M.; Wang, Z. Z.; Chen, X. L.; Yu, B. Y.; Hu, Y. Radiat Phys Chem 2006, 75, 557.
10. Du, L. C.; Qu, B. J.; Xu, Z. J. Polym Degrad Stab 2006, 91, 995.
11. Yang, W. S.; Kim, Y.; Liu, P. K. T.; Sahimi, M.; Tsotsis, T. T. Chem Eng Sci 2002, 57, 2945.
12. Lucrédio, A. F.; Assaf, E. M. J Power Sources 2006, 159, 667.
13. Kantam, M. L.; Kumar, K. B. S.; Raja, K. P. J Mol Catal A 2006, 247, 186.
14. Kuzawa, K.; Jung, Y. J.; Kiso, Y.; Yamada, T.; Nagai, M.; Lee, T. G. Chemosphere 2006, 62, 45.
15. Scavetta, E.; Berrettoni, M.; Giorgetti, M.; Tonelli, D. Electrochim Acta 2002, 47, 2451.
16. Lin, Y. J.; Li, D. Q.; Evans, D. G.; Duan, X. Polym Degrad Stab 2005, 88, 286.
17. Lin, Y. J.; Wang, J. R.; Evans, D. G.; Li, D. Q. J Phys Chem Solids 2006, 67, 998.
18. Nangrani, K. J.; Wenger, R.; Daugherty, P. G. Plast Compd 1988, 11, 2729.
19. Whelan, W. P., Jr. J Fire Ret Chem 1979, 6, 206.
20. Zhu, J.; Wilkie, C. A. Chem Mater 2001, 13, 4649.
21. Weil, E. D.; Pate, N. G. Polym Degrad Stab 2003, 82, 291.